Radiation Measurements 128 (2019) 106181

Contents lists available at ScienceDirect

Radiation Measurements

journal homepage: www.elsevier.com/locate/radmeas

A design study of application of the CsI self-activation method to the neutron rem-counter technique

Taishi Ueki[a,*], Akihiro Nohtomi[a], Genichiro Wakabayashi[b], Junichi Fukunaga[c], Toyoyuki Kato[c], Saiji Ohga[d]

[a] Department of Health Sciences, Kyushu University, 3-1-1 Maidashi, Higashi-ku, Fukuoka, 812-8582, Japan
[b] Atomic Energy Research Institute, Kindai University, 3-4-1 Kowakae, Higashiosaka-shi, Osaka, 577-8502, Japan
[c] Department of Radiology, Kyushu University Hospital, 3-1-1 Maidashi, Higashi-ku, Fukuoka, 812-8582, Japan
[d] Department of Clinical Radiology, Graduate School of Medical Sciences, Kyushu University, 3-1-1 Maidashi, Higashi-ku, Fukuoka, 812-8582, Japan

ARTICLE INFO

Keywords:
CsI self-activation method
Neutron rem-counter technique
Photoneutrons
Medical linacs
Neutron ambient dose-equivalent

ABSTRACT

A design study of application of the CsI self-activation method to the "neutron rem-counter technique" was investigated. A CsI crystal served as both the main target material and 4π counter of neutron activation method in our proposed CsI self-activation method. A commercially available CsI gamma-ray dosimeter was selected as the neutron detector and surrounded with several neutron filters made of polyethylene and silicon rubber containing B_4C. The geometric structure of these neutron filters was optimized by a Monte Carlo calculation to make the neutron response similar to the ICRP-74 rem-response. Optimization of this method, the residual sum of squares (RSS) of the calculated neutron response and the ICRP-74 rem-response were minimized by changing the thickness of each filter sequentially. In addition, experimental verification using a Pu–Be source and photoneutrons from a 10 MV-X medical linac has been conducted. From these results, it is concluded that it may be practical for evaluating neutron ambient dose-equivalent simply around medical linacs.

1. Introduction

It is known that photoneutrons are generated in radiotherapeutic treatment with high-energy medical linacs (National Council of Radiation Protection and Measurements, 1984) (Kryet al., 2017). The photoneutron generation caused by photonuclear reaction between high-Z materials and high-energy X-rays will occur if the X-ray energy exceeds a threshold level (Kryet al., 2017). Such photoneutrons are undesirable to be irradiated to patients, because secondary cancer may be caused owing to their high biological effectiveness (Kryet al., 2017). The amount of generation might depend on the treatment plan for each patient. Therefore, it would be beneficial to measure the neutron ambient dose-equivalent for each patient.

In our previous works, we have proposed high-sensitive neutron detection using the self-activation of an iodine-containing scintillator (Wakabayashiet al., 2015) (Nohtomi and Wakabayashi, 2015) (Nohtomiet al., 2016a) (Nohtomiet al., 2016b). For 10 MV-X medical linacs, for instance, an evaluation of neutron ambient dose-equivalent using a CsI scintillator with several neutron-filtering conditions was successfully conducted. However, the procedure is rather complicated and time-consuming, because the use of several filtering conditions is essential to determine the neutron energy spectrum. Therefore, such an evaluation method is impractical for daily quality assurance purposes.

A neutron rem-counter, whose neutron response is made as close as possible to the ideal ICRP-74 rem-response (ICRP, 1996), has been widely selected as a real-time monitoring system of neutron ambient dose-equivalent (Nakamuraet al., 1985). However, it has been reported that employment of the rem-counter around medical linacs is unfavorable, because an active-type detector in the rem-counter often shows malfunctions at pulsed neutron radiation fields (Odaet al., 1985). A passive-type detection such as our proposed method is more appropriate in this case. Thus, in the present work, a design study of application of the CsI self-activation method to the "neutron rem-counter technique" (Nakamuraet al., 1985) was investigated. Specifically, we used a CsI scintillator as a thermal neutron detector based on the self-activation method and the scintillator was surrounded with optimized neutron filters. Such application might be useable even for medical linacs. In this design, the geometric structure of the thermal neutron detector and neutron filters was optimized by a Monte Carlo calculation to become a neutron response similar to the ICRP-74 rem-response. Subsequently, we manufactured a rem-counter with the CsI self-activation method (the present neutron dosimeter) as a trial and conducted

* Corresponding author.
E-mail address: taa.ueki@gmail.com (T. Ueki).

https://doi.org/10.1016/j.radmeas.2019.106181
Received 25 March 2019; Received in revised form 7 July 2019; Accepted 13 August 2019
Available online 19 August 2019
1350-4487/

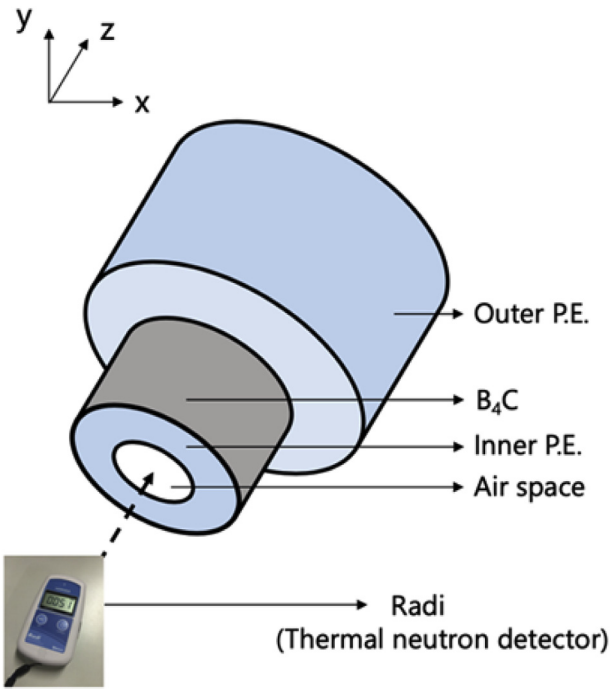

Fig. 1. Geometrical structure of the present neutron dosimeter.

experimental verification with Pu–Be and photoneutron sources to confirm the operating characteristics.

2. Design of the present neutron dosimeter

The present neutron dosimeter was designed by using a commercially available CsI gamma-ray dosimeter (Radi PA-1100 made by HORIBA (Radi PA-1100, 1100)), which has a wireless communication interface making the remote acquisition of data possible. This is a great advantage in practical use. The Radi was used as a thermal neutron detector employing the CsI self-activation method. We positioned a CsI scintillator of the Radi almost at the center of the dosimeter. The neutron filters, which surround the Radi, were made of polyethylene (P.E.) and silicon rubber containing 50 wt% B_4C (B_4C). P.E. and B_4C were used as the neutron moderator and absorber, respectively. A cylindrical structure was adopted for the neutron filters to reduce the directional dependency of the neutron response. A spherical structure would have been preferable; however, such a structure was not selected owing to difficulty of manufacturing. These neutron filters consist of three layers: an Outer P.E., Inner P.E., and a B_4C as shown in Fig. 1.

The thicknesses of the moderator and absorber were determined by a Monte Carlo calculation called Particle and Heavy Ion Transport code System validation (PHITS) (Satoet al., 2018). The PHITS calculation was performed to make the neutron response similar to the ICRP-74 rem-response, especially in the energy range from 100 keV to 10 MeV. We utilized the residual sum of squares (RSS) for examining the matching degree between the neutron response and the ICRP-74 rem-response. The RSS was minimized by changing the thickness of each filter sequentially. The RSS is expressed by Eq. (1),

$$RSS = \sum_i \left((R_{\mathrm{rem}}(E))_i - (R_{\mathrm{cal}}(E))_i \right)^2 \quad (1)$$

where $(R_{\mathrm{rem}}(E))_i$ is the normalized ICRP-74 rem-response and $(R_{\mathrm{cal}}(E))_i$ is the normalized neutron response calculated by PHITS.

From the results of the evaluation of RSS (Figs. 2 – 4), the optimized thicknesses of the Outer P.E. and Inner P.E. were determined to be 7.0 cm and 1.5 cm, respectively. The B_4C was determined to be 1.5 mm thickness. In addition, to house the Radi, a cylindrical space with radius

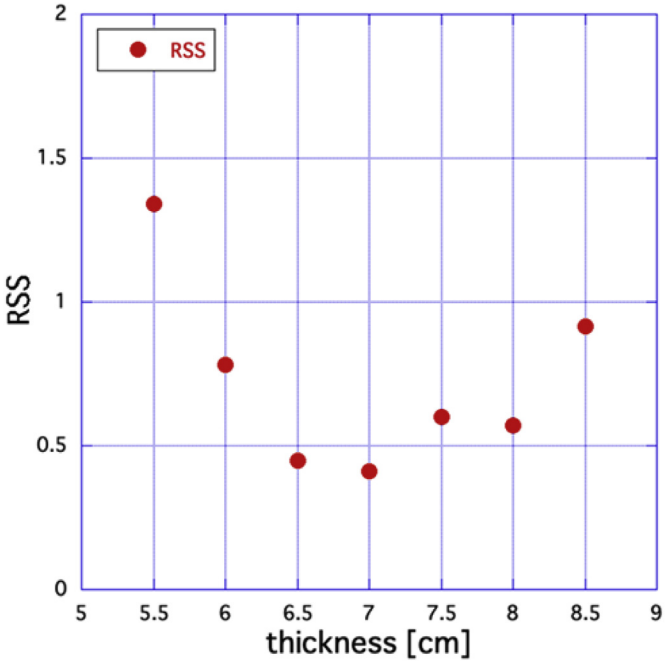

Fig. 2. RSS for Outer P.E.

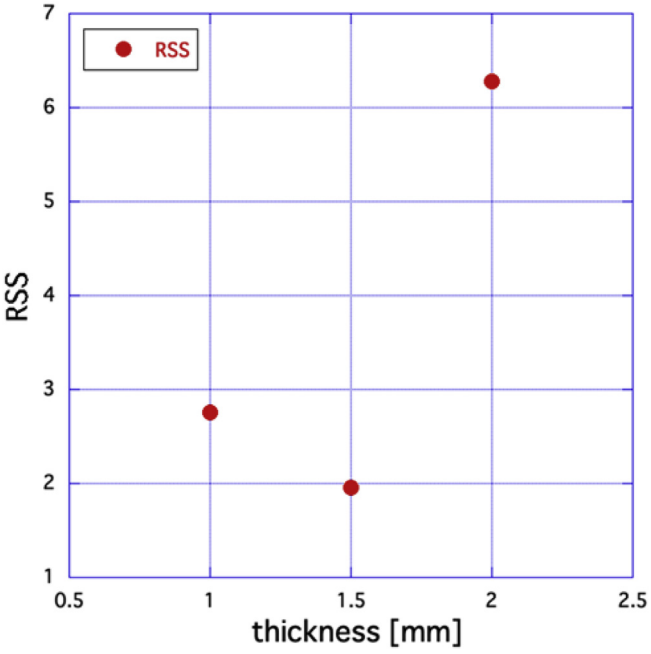

Fig. 3. RSS for B_4C.

3.6 cm was arranged. Consequently, the overall dimensions of the present neutron dosimeter were 25.0 cm diameter and 20.9 cm length. We summarized the primary size specification in Table 1.

Fig. 5 shows the optimized neutron response of the present neutron dosimeter. It was rather well fitted to the ICRP-74 rem-response (energy range 10^{-9} to 10^{1} MeV). Fig. 6 is a more detailed comparison between the ratios of the optimized neutron response and the ICRP-74 rem-response. The matching degree of responses in the fast neutron region (energy range 10^{-1} to 10^{1} MeV) was the most important element in this design study, because fast neutrons generally have the highest biological effectiveness. By contrast, notable deviation from the ICRP-74 rem-response was observed, especially in the thermal and epithermal neutron regions (energy range 10^{-9} to 10^{-2} MeV). However,

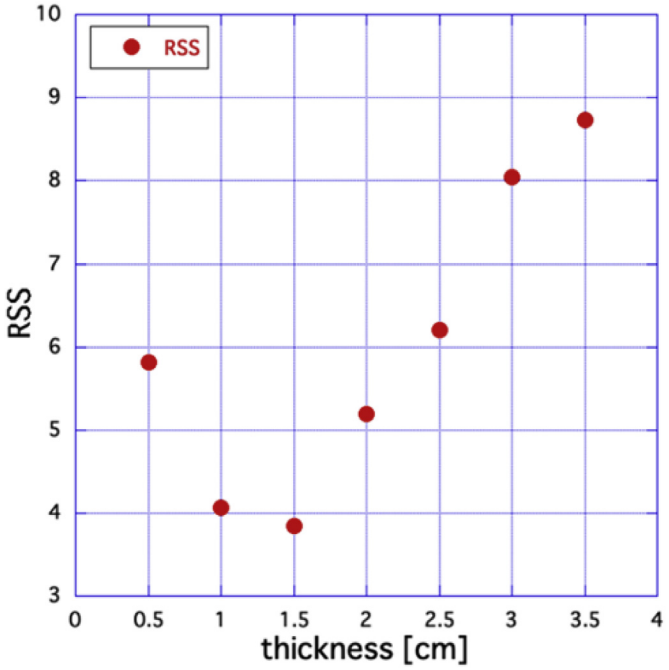

Fig. 4. RSS for Inner P.E.

Table 1
Primary size specification of the present neutron dosimeter.

Neutron Filters	Size (cm)
Thickness of Outer P.E.	7.0
Thickness of Inner P.E.	1.5
Thickness of B_4C	0.15
Radius of cylindrical space	3.6
Overall dimensions	$\phi 25 \times 20.9$

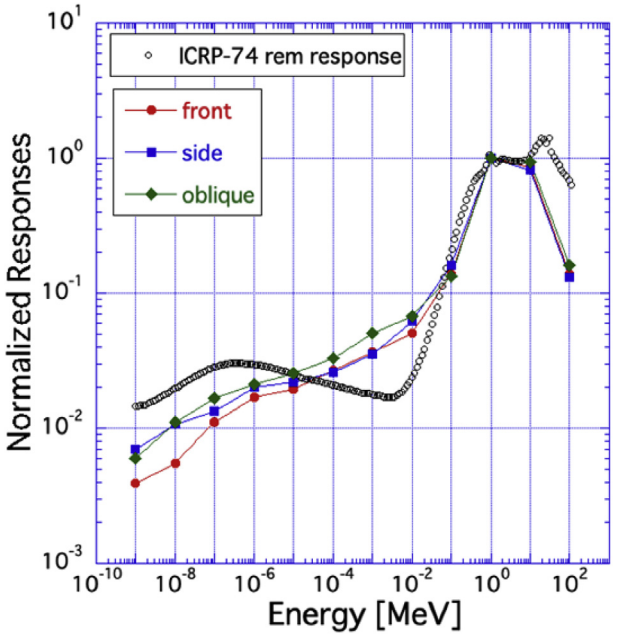

Fig. 5. The optimized neutron response and ICRP-74 rem-response. The meaning of "front," "side," and "oblique" in the curves is direction of neutron irradiation in PHITS (from 0°, 45°, and 90°, respectively).

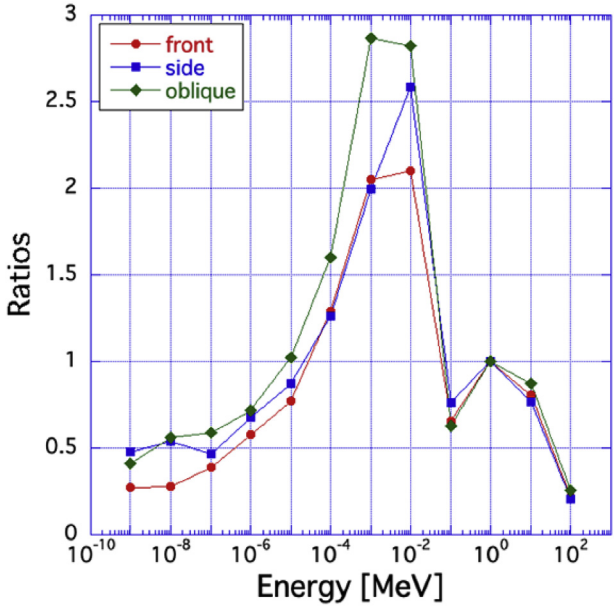

Fig. 6. Ratios of the optimized neutron response and ICRP-74 rem-response.

the maximum deviation is lower than a factor of 3. This result is not inferior compared to the response of the rem-counter realized by Nakamura et al. (Nakamuraet al., 1985). It is confirmed that the present neutron dosimeter shows a small difference in directional dependency between "front" and "oblique" in the epithermal region. This is caused by the cylindrical shape of the neutron filters. When we consider the shape difference between the present dosimeter and the rem-counter, the directional dependency may be kept within an acceptable level. From these facts, the present neutron dosimeter has a practical neutron response.

As a trial, as shown in Fig. 7, we manufactured the present neutron dosimeter based on the optimized design.

3. Determination of a conversion factor for the present neutron dosimeter

A conversion factor f (mSv/h/Bq) of the present neutron dosimeter was determined, which converts ^{128}I saturated activities A_{sat} (Bq) evaluated by using the CsI self-activation method into neutron ambient dose-equivalent $H^*(10)$ (mSv/h). In this work, f is obtained by following Eq. (2),

$$f = \frac{\int_0^\infty h^*(E)\phi(E)dE}{\int_0^\infty R(E)\phi(E)dE} = \frac{H^*(10)}{A_{sat}} \quad (2)$$

where E is the neutron energy (eV), $\phi(E)$ is the neutron fluence rate (n/

Fig. 7. The present neutron dosimeter.

Table 2
The conversion factors (mSv/h/Bq) derived in various medical linacs.

	Medical linac field				
	Field 1	Field 2	Field 3	Field 4	Field 5
front	0.0553 ± 0.0016	0.0552 ± 0.0015	0.0534 ± 0.0003	0.0620 ± 0.0083	0.0503 ± 0.0034
side	0.0519 ± 0.0018	0.0538 ± 0.0001	0.0506 ± 0.0031	0.0557 ± 0.0020	0.0484 ± 0.0053
total	0.0537 ± 0.0027				

cm^2/s), $h^*(E)$ is the ICRP-74 rem-response (mSv cm^2), and $R(E)$ is the neutron response (cm^2).

The denominator component A_{sat} can be specifically expressed as follows:

$$A_{sat} = \phi N \sigma V S \quad (3)$$

where ϕ is the neutron fluence rate ($n/cm^2/s$), N is the number density of iodine atoms in the CsI scintillator ($1/cm^3$), σ is the neutron capture cross-section of the reaction ^{127}I (n, γ) ^{128}I (cm^2), V is the volume of the CsI scintillator (cm^3), and S is the self-shielding correction factor. The values of σ and S in Eq. (3) depend on the neutron energy and the detector dimensions. Thus, A_{sat} in the CsI scintillator can be calculated if the neutron energy spectrum is already known, and was calculated by PHITS. For this purpose, in our PHITS calculation, we used the reference data reported by Domingo et al. (Domingoet al., 2010). Domingo et al. performed neutron spectrometry and dosimetry at various medical linacs (Field 1 – Field 5). The reference $H^*(10)$ and the calculated A_{sat} were used to derive conversion factors by following Eq. (2). Finally, as an average of those results, f was determined to be 0.0537 ± 0.0027 (mSv/h/Bq) (Table 2). As a general observation, the shapes of the energy spectra of photoneutrons are practically unchanged at each energy region and only the ratio between them varies with the irradiation condition (Nohtomiet al., 2016a). Thus, f mainly includes such tendency. The present neutron dosimeter can show $H^*(10)$ with good accuracy if only f is applied for the evaluation in such fields.

4. Experimental verification of operating characteristics at two neutron fields

4.1. Performance test using a Pu–Be source

Preliminary experiments using a Pu–Be source (37 GBq) at the Atomic Energy Research Institute of Kindai University were conducted to confirm operating characteristics of the present neutron dosimeter. Fig. 8 shows a schematic top view of the experimental setup. The Pu–Be source was positioned at 12.5 cm and 17.7 cm from the center of CsI

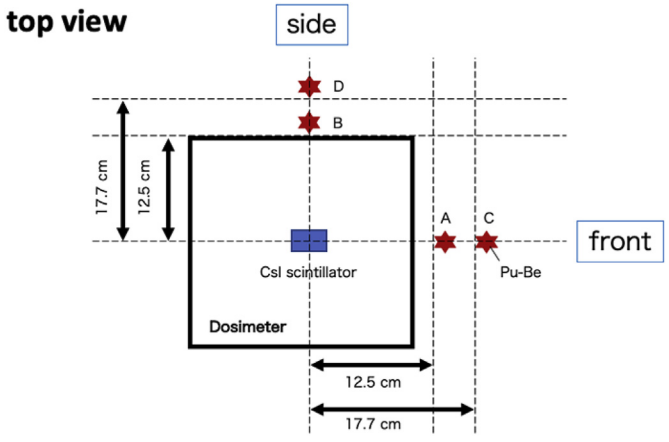

Fig. 8. The schematic top view of the experimental setup.

Table 3
$H^*(10)$ of Pu–Be source were evaluated and summarized. $H^*(10)_{A.}$, $H^*(10)_{B.}$, $H^*(10)_{C.}$, and $H^*(10)_{D.}$ were measured at the A, B, C, and D position in Fig. 8, respectively.

	$H^*(10)_{A.}$ (mSv/h)	$H^*(10)_{B.}$ (mSv/h)	$H^*(10)_{C.}$ (mSv/h)	$H^*(10)_{D.}$ (mSv/h)
Pu–Be	3.27 ± 0.51	2.58 ± 0.45	1.44 ± 0.33	1.20 ± 0.30

crystal of Radi (Position A, B, C, D in Fig. 8). After irradiations of 75 min, the Radi with the activated CsI scintillator was connected to a PC with a wireless communication and data was collected. ^{128}I initial activities A_0 were estimated by fitting the observed decay curve with exponentially decaying components having half-life of 25 min (^{128}I) and 174 min (^{134m}Cs). ^{128}I saturated activities A_{sat} were calculated by using the estimated A_0, and finally converted into neutron ambient dose-equivalent $H^*(10)$ by the conversion factor f. $H^*(10)$ measured at each position is summarized in Table 3.

We plotted $H^*(10)_{ave.}$ and $H^*(10)_{rem.}$, which were respectively the average values of the $H^*(10)$ and the measurement values by a rem-counter (NSN2 (NSN2, 2019)) at 7.0, 12.5, 17.7, 30.0, 50.0, and 80.0 cm from the Pu–Be source, in Fig. 9. The values of $H^*(10)_{ave.}$ tend to be higher compared with that of $H^*(10)_{rem.}$. However, the difference is small, and the values of $H^*(10)_{ave.}$ as well as $H^*(10)_{rem.}$ follow the inverse square law of the distance expressed as a black broken line. This tendency indicates that the present neutron dosimeter has high reliability. Consequently, the present neutron dosimeter normally worked as expected and the directional dependency in each direction was smaller than 20%. For example, although a high-sensitive rem-counter realized by T. Nakamura et al. (Nakamuraet al., 1985) had a superior directional dependency within 10%, considering the difference in geometric

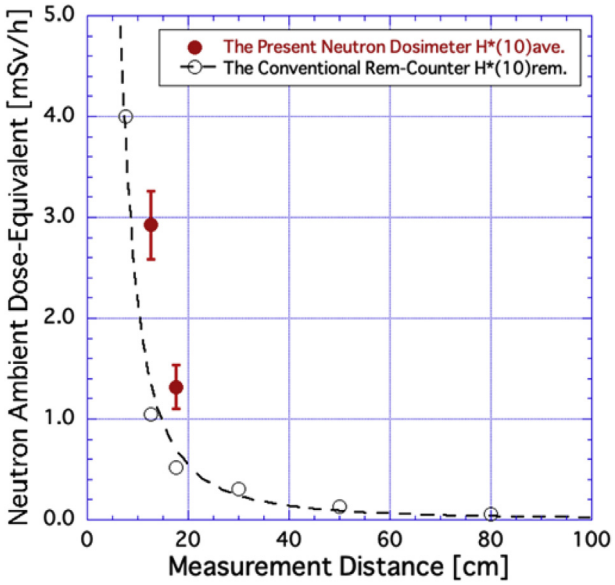

Fig. 9. H*(10)ave. and H*(10)rem. are following the inverse square law of the distance expressed as a black broken line.

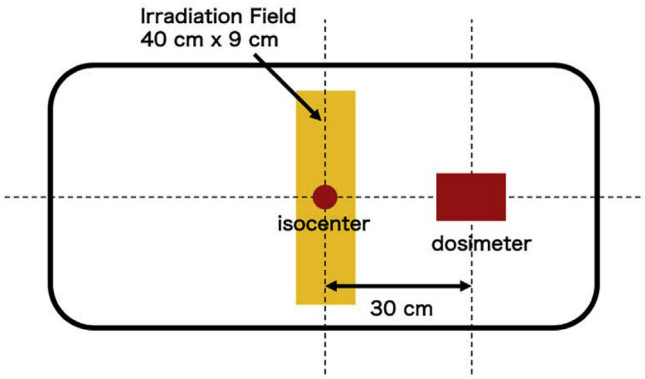

Fig. 10. The schematic layout of the experiment at a 10 MV-X medical linac.

Table 4
$H^*(10)$ at a 10 MV-X medical linac were evaluated and summarized. $H^*(10)_{pre.}$ was evaluated in our previous work. $H^*(10)_{exp1.}$ and $H^*(10)_{exp2.}$ were evaluated in the present work.

	$H^*(10)_{pre.}$ (mSv/Gy$_x$)	$H^*(10)_{exp1.}$ (mSv/Gy$_x$)	$H^*(10)_{exp2.}$ (mSv/Gy$_x$)	$\varepsilon_{exp1.}$	$\varepsilon_{exp2.}$
Varian TrueBeam	0.054	0.081 ± 0.0082	0.081 ± 0.0082	1.5	1.5

structures between dosimeters, our dosimeter is acceptable practically.

4.2. Performance test at a medical linac

Experiments were conducted at a 10 MV-X medical linac (Varian TrueBeam) at the Kyushu University Hospital. The operational condition was for a total-body irradiation with a field size of 40 cm × 9 cm, and the dose rate was 3 Gy/min at the isocenter. A schematic layout of the experiment is shown in Fig. 10. After the irradiation of 30 min, we analyzed the generated activities in the CsI scintillator and finally the neutron ambient dose-equivalent $H^*(10)$ was evaluated. We conducted the same experiments twice to verify reproducibility. Table 4 shows the results of the $H^*(10)$ evaluation.

The deviation between the first experiment and the second was sufficiently small, and it demonstrates good reproducibility of the evaluations by the present neutron dosimeter. The values of $\varepsilon_{exp1.}$ and $\varepsilon_{exp2.}$ in Table 4 represent the relative errors of the present measurement to the experimental measurement under the same conditions conducted in our previous work (Kakino, 2018). These were within 1.5. According to M. Sasaki et al., a neutron dosimeter is typically judged to be useful if the change of measurements in various neutron fields is within a factor 2 margin of accuracy (Sasakiet al., 1998). Based on this report, the present neutron dosimeter can be judged useful, and we can judge that the present neutron dosimeter has a practical performance around medical linacs.

5. Conclusion

A design study of application of the CsI self-activation method to the neutron rem-counter technique was investigated and the optimized neutron response closely resembled the ICRP-74 rem-response from 10^{-1}–10^{1} MeV. The performance of a newly designed neutron dosimeter was experimentally verified. It worked not only in a Pu–Be field but also in a pulsed radiation field such as those around medical linacs. In particular, the accuracy of the measurements around medical linacs certifies usefulness of the present neutron dosimeter. Although an exact discussion is difficult, one concern is that the neutron sensitivity of the present neutron dosimeter is approximately 3–20 times smaller than that of commercially available cylindrical rem-counters (Nakamuraet al., 1985). If the neutron dose is lower than the value of 0.081 (mSv/Gy$_x$) measured in the present experiment, the CsI scintillator positioned in the dosimeter is not sufficiently activated and it results in uncertain measuring of the neutron dose. Nevertheless, at least, we can use the dosimeter to check whether the neutron ambient dose-equivalent is within an acceptable level. In conclusion, it is expected that the present neutron dosimeter is practical for monitoring the neutron radiation around medical linacs.

Conflicts of interest

The authors declare that they have no conflict of interest.

Acknowledgements

This study was performed in part under the Cooperative Research at Kindai University Reactor supported by the Graduate School of Engineering, Osaka University. The authors thank Mr. R. Kurihara and Ms. Y. Hanada of the Department of Health Sciences, Kyushu University, for their cooperation in the experiments, and also Mr. H. Ito of the HORIBA for his provision of information regarding Radi PA-1100.

References

Domingo, C., et al., 2010. Neutron spectrometry and determination of neutron ambient dose equivalents in different LINAC radiotherapy rooms. Radiat. Meas. 45, 1391–1397.
ICRP, 1996. Conversion coefficients for use in radiological protection against external radiation. ICRP Publication 74. Ann. ICRP 26 (3–4).
Kakino, R., 2018. Development of Neutron Dose Evaluation Method during Radiation Therapy by Using the Self-Activation of a CsI Scintillator. master's thesis. Department of Health Sciences, Kyushu University.
Kry, Stepen F., et al., 2017. Measurement and calculation of doses outside the treated volume from external-beam radiation therapy. AAPM TG 158.
Nakamura, T., et al., 1985. realization of a high sensitivity neutron rem counter. Nucl. Instrum. Methods Phys. Res. 241, 554–560.
National Council of Radiation Protection and Measurements, 1984. Neutron contamination from medical electron accerators. NCRP (Natl. Counc. Radiat. Prot. Meas.) Rep. 79.
Nohtomi, A., Wakabayashi, G., 2015. Accuracy of neutron self-activation method with iodine-containing scintillators for quantifying I-128 generation using decay-fitting technique. Nucl. Instrum. Methods Phys. Res. 800, 6–11.
Nohtomi, A., et al., 2016a. Proc. Int. Symp. On radiation detectors and their uses (ISRD2016). JPS Conf. Proc. 11, 050002. https://doi.org/10.7566/JPSCP.11.050002.
Nohtomi, A., et al., 2016b. An application of CCD read-out technique to neutron distribution measurement using the self-activation method with a CsI scintillator. Nucl. Instrum. Methods Phys. Res. A 832, 21–23.
NSN2 Fuji electric. [Online]. Available. https://www.fujielectric.co.jp/products/radiation/servy/nsn/ Accessed 11 3 2019.
Oda, K., et al., 1985. Evaluation of neutron dose equivalent in pulsed and mixed radiation field around electron linear accelerator with rem-counter. Health Sci. Phys. 20, 371–378.
Radi PA-1100 HORIBA. [Online]. Available. http://www.horiba.com/jp/process-environmental/products-jp/environmental-radiation-monitor/details/pa-1100-radi-environmental-radiation-monitor-with-communications-function-16189/ Accessed 11 3 2019.
Sasaki, M., et al., 1998. Development and characterization of real-time personal neutron dosemeter with two silicon detectors. Nucl. Instrum. Methods Phys. Res. 418, 465–475.
Sato, T., et al., 2018. Features of Particle and Heavy Ion Transport code system (PHITS) version 3.02. J. Nucl. Sci. Technol. 3131, 1–7.
Wakabayashi, G., et al., 2015. Applicability of self-activation of an NaI scintillator for measurement of photo-neutrons around a high-energy X-ray radiotherapy machine. Jpn. Soc. Radiol. Technol. Japan Soc. Med. Phys. 8, 125–134.